Two MYB activators of anthocyanin biosynthesis exhibit specialized activities in petiole and fruit of diploid strawberry

Xi Luo<sup>1,†</sup>, Madison Plunkert<sup>1,†</sup>, Zi Teng<sup>2</sup>, Kathryn Mackenzie<sup>3</sup>, Lei Guo<sup>1</sup>, Yaguang Luo<sup>2</sup>, Timo Hytönen<sup>3</sup>, and Zhongchi Liu<sup>1\*</sup>

1. Dept. of Cell Biology and Molecular Genetics, University of Maryland, College Park, MD, USA

2. Food Quality Lab/Environmental Microbial and Food Safety Lab, USDA, ARS, NEA, BARC, FQL/EMFSL, Beltsville, MD, USA

3. Department of Agricultural Sciences, Viikki Plant Science Centre, University of Helsinki, Helsinki, Finland

†: equal contribution

\*: corresponding author (zliu@umd.edu)

Xi Luo: xiluo@umd.edu

Madison Plunkert: mlplunkert@gmail.com

Zi Teng: davidtzfe@gmail.com

Kathryn Mackenzie: kathryn.mackenzie@helsinki.fi

Lei Guo: guo@umd.edu

Yaguang Luo: yaguang.luo@usda.gov

Timo Hytönen: timo.hytonen@helsinki.fi

#### Highlight

Strawberry plants accumulate anthocyanin pigments in petioles through the action of *FveMYB10-Like*. Unlike *FveMYB10, FveMYB10-Like* expression is repressed in shade and *FveMYB10-Like* shows different preference for downstream target genes.

© The Author(s) 2022. Published by Oxford University Press on behalf of the Society for Experimental Biology. All rights reserved. For permissions, please email: journals.permissions@oup.com

#### Abstract

The R2R3-MYB transcription factor FveMYB10 is a major regulator of anthocyanin pigmentation in the red strawberry fruits. *fvemyb10* loss-of-function mutants form yellow fruits but still accumulate purple-colored anthocyanins in the petioles, suggesting that anthocyanin biosynthesis is under distinct regulation in fruits and petioles. We identified a *green petioles* (*gp*)-1 mutant from chemical mutagenesis in the diploid wild strawberry *Fragaria vesca* that lacks anthocyanins in petioles. Using mapping-by-sequencing and transient functional assays, we confirmed that the causative mutation resides in a *FveMYB10-Like* (*MYB10L*) gene and that *FveMYB10* and *FveMYB10L* function independently in the fruit and petiole respectively. In addition to their tissue-specific regulation, *FveMYB10* and *FveMYB10L* respond differently to changes in light quality, produce distinct anthocyanin compositions, and preferentially activate different downstream anthocyanin biosynthesis genes in their respective tissues. This work identifies a new regulator of anthocyanin synthesis and demonstrates that two paralogous MYB genes with specialized functions enable tissue-specific regulation of anthocyanin biosynthesis in fruit and petiole tissues.

**Keywords:** anthocyanin, diploid wild strawberry, *Fragaria vesca*, fruit, *MYB10*, *MYB10-Like*, petiole, tissue-specific regulation,

#### Introduction

Anthocyanins are a class of flavonoid pigments widely found in plants (Tanaka *et al.*, 2008). Abundantly present in flowers and fruits, anthocyanins help attract pollinators and seed dispersers (Lomascolo *et al.*, 2010; Landi *et al.*, 2015). In vegetative tissues, anthocyanins are produced to enhance plant tolerance of a variety of abiotic and biotic stresses (Chalker-Scott, 1999; Li *et al.*, 2017; Nevo *et al.*, 2018). When consumed, anthocyanins offer significant benefit to human health, ranging from protection against cardiovascular diseases and cancer to suppressors of inflammatory pathways (Kong *et al.*, 2003; Zhang *et al.*, 2014). Plant products that are rich in anthocyanins are more attractive to consumers due to the bright and beautiful colors as well as high antioxidant levels (King and Cliff, 2002; Pojer *et al.*, 2013). Therefore, increasing anthocyanin content is a major goal for crop improvement (Zhu *et al.*, 2017; Sun *et al.*, 2020).

Anthocyanin biosynthesis occurs through the well-characterized flavonoid pathway, which begins with the sequential action of chalcone synthase (CHS), chalcone isomerase (CHI), and flavanone 3β-hydroxylase (F3H) to synthesize dihydroflavonols. The enzymes F3'H and F3'5'H produce dihydroflavonols with different hydroxylation states, which will affect the hue of the anthocyanins produced (Berardi *et al.*, 2021). Dihydroflavonol 4-reductase (DFR) catalyzes the first committed step for producing anthocyanidins instead of flavonols. Anthocyanidin reductase (ANR) and UDP-glucosyltransferases (UFGTs) then act sequentially to synthesize anthocyanins (Xu *et al.*, 2014). Anthocyanin biosynthesis genes are activated by the MBW transcriptional activation complex, composed of an R2R3-MYB transcription factor, a basic-helix-loop-helix (bHLH), and a WD-repeat protein (Xu *et al.*, 2015). MBW complexes regulate many processes in plants, with the R2R3-MYB protein often specifying the regulatory targets of the complex (Heppel *et al.*, 2013).

Strawberry (*Fragaria* × *ananassa*, octoploid) is an economically important fruit crop worldwide. The wild strawberry *Fragaria vesca*, the diploid progenitor for the dominant subgenome in *F*. × *ananassa*, has been used as a model system for strawberry and the Rosaceae family, due to its diploidy, high quality genome, ever-flowering accessions, small stature, and available molecular genetic tools (Zhou *et al.*, 2018; Edger *et al.*, 2018; Liu *et al.*, 2020; Gaston *et al.*, 2020). The attractive red color of strawberry fruit has led to extensive research, which revealed *FveMYB10*, an R2R3-MYB, playing a critical role in controlling the biosynthesis of anthocyanins in strawberry fruit. Multiple natural variations in the *MYB10* coding or regulatory sequences underlie white fruit skin or

cortex of both F.  $\times$  ananassa and F. vesca (Castillejo et al., 2020). FaMYB10 and FveMYB10 expressions increase as fruit ripens (Lin-Wang et al., 2010). Furthermore, RNAi down-regulation of MYB10 in F.  $\times$  ananassa and F. vesca respectively reduces or eliminates anthocyanins in fruits (Lin-Wang et al., 2014; Medina-Puche et al., 2014).

Strawberry also accumulates anthocyanins in the vegetative tissues, most visibly in the petioles. Most white-fruited *F. vesca* accessions, such as 'Yellow Wonder (YW)' and 'Hawaii 4 (H4)', carry *myb10* mutations (Hawkins *et al.*, 2016; Castillejo *et al.*, 2020), yet they still develop purple-colored petioles, indicating that anthocyanins are produced normally in the petioles and regulated independently of *FveMYB10*. Hence, anthocyanin biosynthesis in fruit and petiole must be regulated by different genetic factors, prompting the hypothesis that a different R2R3-MYB in strawberry might regulate anthocyanin biosynthesis in the petioles. However, the identity of such an R2R3-MYB remains elusive. Previously, a *reduced anthocyanins in petioles* (*rap*) mutant of *F. vesca* was identified; the causal mutation resides in a GST gene coding for the glutathione S-transferase needed to transport anthocyanins from the cytosol to the vacuole in petioles and fruits. As a result, *rap* mutants exhibit reduced pigmentation in fruit as well as in petiole (Luo *et al.*, 2018). Hence, it is unlikely that *RAP* encodes the unknown factor specific for the petioles.

Here, we report the isolation and characterization of a *green petioles* (*gp*)-1 mutant in the wild strawberry *F. vesca*. Mapping-by-sequencing identified the causal mutation in an R2R3-MYB gene that is similar in sequence to *FveMYB10*. This new gene is named *FveMYB10-Like* (*FveMYB10L*). Phylogenetic and functional analyses showed that, like FveMYB10, FveMYB10L is also an activator of anthocyanin biosynthesis, but unlike FveMYB10, FveMYB10L is specifically required for anthocyanin synthesis in the petiole, hence fulfilling the role of the elusive R2R3-MYB for petiole-specific anthocyanin synthesis. Further, *FveMYB10* and *FveMYB10L* expression was shown to respond differently to light quality, and ectopic activation of *FveMYB10L* in fruits induces a distinct anthocyanin profile resembling that of wild-type petioles and shows different activation capability of anthocyanin biosynthesis genes from *FveMYB10*. Our work demonstrates the existence of separate genetic controls for fruit and petiole anthocyanin biosynthesis and identifies the transcription factors that exert such separate controls. The *FveMYB10* and *FveMYB10L* genes offer flexible regulation of anthocyanin accumulation under different developmental and environmental conditions.

#### **Materials and Methods**

# Plant material and growth conditions

The seventh-generation inbred lines of F. vesca accessions Rügen (Rü, red fruits and purplish petioles), Yellow Wonder 5AF7 (YW, white fruits and purplish petioles), and Hawaii 4 (H4, white fruits and purplish petioles) (Hawkins et~al., 2016; Joldersma et~al., 2022) were used in this study. The natural accession FIN12 lacks anthocyanins in all tissues and was collected from southern Finland (WGS84 N60.15, E21.59). The rap-1 is from Dr. Chunying Kang (Luo et~al., 2018). gp-1 was obtained from chemical mutagenesis by N-ethyl-N-nitrosourea (ENU) in a YW genetic background. ENU mutagenesis produces point mutations, mainly affecting A/T base pairs, and can produce both transitions and transversions (Justice et~al., 1999). The mutagenesis was previously described (Caruana et~al., 2018). Briefly, YW seeds were treated with 4mM ENU for four hours. Seeds were then rinsed with water, plated on MS media, and cold-treated for 5 weeks to induce germination. The gp-1 mutant was identified in the M2 generation. The plants were cultivated in a growth chamber under white light, provided by Phillips F32T8/TL841 linear fluorescent bulbs, with light intensity of 110  $\mu$ mol m<sup>-2</sup> s<sup>-1</sup> and a 13/11 h light/dark photoperiod at 23 °C.

# **Complementation tests**

Reciprocal crosses between *gp-1* and *rap-1* were performed and F1 individuals with purple petioles were observed, indicating complementation between *gp-1* and *rap-1*.

Pollen from *gp-1* was used to pollinate the stigma of FIN12. To prevent self-fertilization, the flowers were emasculated before the dehiscence of anthers. The plants were covered and new open flowers removed until fruit development. The seeds were germinated and all of the 46 F1 seedlings were examined at the four-leaf stage and shown to develop green petioles, indicating that *gp-1* and FIN12 mutations are allelic.

# Mapping the gp-1 mutation through bulk-segregant analysis

The *gp-1* mutant was crossed with H4 that possesses wild-type purplish petioles, and a single F1 plant was self-fertilized to produce the F2 mapping population. Petiole color was scored in the F2 population, and genomic DNA was pooled from 25 green petiole individuals and from

25 purple petiole individuals to produce the mutant and wild-type pools respectively. Genomic DNA was extracted with DNAEasy Power Plant Pro kit (Qiagen, USA) or NucleoSpin Plant II kit (Macherey-Nagel, USA), followed by cleanup with the NucleoSpin Genomic DNA Cleanup kit (Macherey-Nagel, USA). The two DNA pools were sequenced using the Illumina NovaSeq 6000 System (Novogene, Sacramento, USA).

A total of 106.5 and 107.9 million paired-end 150 bp reads respectively from *gp-1* and wild-type were filtered using fastp (Chen *et al.*, 2018) to remove low quality reads. Afterwards, 105.9 high-quality mutant and 107.3 high-quality wild-type reads were retained for downstream analysis. Candidate *gp-1* mutations were identified using the SIMPLE pipeline (Wachsman *et al.*, 2017). Briefly, SIMPLE maps sequencing reads to a reference genome, calls SNPs between the mutant and wild type bulks, and identifies candidate SNPs expected to affect gene function. Those variants for which no reference reads occur in the mutant pool and the wild-type pool has about 2/3 reference reads are identified as candidates. Since ENU mutagenesis cannot cause indels, indels were removed from the list of candidates. Known variants occurring in the accessions YW, H4, and Rü, all of which have purplish petioles, were identified by mapping their sequencing reads derived from a previous study (Hawkins *et al.*, 2016) against the *F. vesca* reference genome (Edger *et al.*, 2018; Li *et al.*, 2019). Variants were called using the mapping and variant calling approaches in the SIMPLE pipeline. SNPs that are expected to affect gene function as a missense, nonsense, or splicing variant not known to occur in YW, H4, or Rü genome, as well as any SNPs residing in genes expected to affect anthocyanin biosynthesis, were selected as candidates.

# Phylogenetic analysis of FveMYB10L

Protein sequences in *Arabidopsis* and tomato from R2R3-MYB subgroup 6, which regulates anthocyanin biosynthesis, and related subgroups 5, 7, and 15 were identified based on a recent phylogenetic analysis that placed these subgroups in a clade with subgroup 6 (Rodrigues *et al.*, 2021) and downloaded from TAIR and Sol Genomics Network (Fernandez-Pozo *et al.*, 2015; Berardini *et al.*, 2015). Their gene accession numbers are summarized in Table S1. Multiple sequence alignment containing these sequences, FveMYB10, and FveMYB10L, as well as OsGAMYB as an outgroup, was created using the MUSCLE algorithm implemented in MEGA X software (Edgar, 2004; Stecher *et al.*, 2020). The rooted maximum likelihood tree was constructed using the James Taylor Thornton matrix-based model with 1000 bootstrap replicates (Jones *et al.*, 1992). The pairwise sequence alignment of the FveMYB10 and FveMY10L protein sequences was made using the Needleman-

Wunsch algorithm implemented in EMBL-EBI (Madeira *et al.*, 2022). The gene IDs of the genes used in this study are listed in the Supplementary Table S1.

# Construction of FveMYB10L and FveMYB10 overexpression plasmids

The JH23 vector was previously constructed from a gateway cloning vector pMDC99 (Curtis and Grossniklaus, 2003) by adding OCS terminator and the Arabidopsis Ubiquitin 10 (UBQ) promoter (Zhou *et al.*, 2021). To assemble *pUBQ::GFP*, the GFP coding sequence was Gibson assembled into JH23 following KpnI and PacI vector digestion so that GFP is driven by the UBQ promoter. To assemble *pUBQ::FveMYB10L* and *pUBQ::FveMYB10L* R90K plasmids, total RNA was extracted from YW and *gp-1* mutant petioles respectively using the CTAB RNA extraction method (Gambino *et al.*, 2008) and then treated with DNase I (catalog number M303S, New England Biolabs) to remove genomic DNA contamination. cDNAs were synthesized from total RNA using the RevertAid First Strand cDNA Synthesis Kit (catalog number K1622, Thermo Scientific). The mutant and wild-type *FveMYB10L* coding sequences were amplified from the cDNA and respectively cloned into the *pUBQ::GFP* vector following KpnI digestion to produce *pUBQ::FveMYB10L-GFP* or *pUBQ::FveMYB10LR90K-GFP*. All primers used are listed in the Supplementary Table S2.

The *p35S::FveMYB10* overexpression construct was previously described (Hawkins *et al.*, 2016), in which the *FveMYB10* cDNA is driven by the 35S promoter in the pMDC32 vector (Curtis and Grossniklaus, 2003). An empty pMDC32 vector was used as the control for *p35S::FveMYB10* in the fruit transient expression assay.

# Transient expression assay using strawberry fruit

Transient expression assays in wild diploid strawberry fruit were performed as described by Hawkins et~al.~(2016) with minor modifications. Agrobacterium~tumefaciens strain GV3101 containing an overexpression or control construct was grown in 3 ml LB liquid medium with 50 mg/ml kanamycin overnight at 28 °C incubator. The culture was resuspended in Murashige and Skoog medium with 2% (w/v) sucrose to an exact OD<sub>600</sub> of 1.0. White stage fruits were identified for injection based on morphological cues, including visible spaces between achenes, the white color of the achenes and receptacle, and approximate age since flower anthesis (Hawkins et~al., 2017). A 1 ml insulin syringe was used in injection until the fruit appeared saturated with the infiltration solution (~50  $\mu$ l). At least 12 fruits were infiltrated for each construct. Fruits were removed from the plants at maturity (~5-10 days after the injection) and photographed.

# **Anthocyanin analyses**

Mature fruits transiently expressing *pUBQ::FveMYB10L*, *pUBQ::FveMYB10L*<sup>R90K</sup>, or control vector *pUBQ::GFP* were frozen in liquid nitrogen. Total anthocyanin extraction and measurement was performed in three replicates according to Luo *et al.* (2018). Briefly, fresh tissue was ground in liquid nitrogen and combined with 5 ml of extraction solution (70 parts methanol: 27 parts water: 2 parts formic acid: 1 part trifluoroacetic acid). After incubating in the dark at 4°C for 12h, the supernatant was transferred to a new tube and absorbance measured with Nanodrop 2000c at 530 nm and 657 nm to quantify total anthocyanins. Anthocyanin content was calculated as [A530–(0.25×A657)]/M, where A530 and A657 are the absorbance at the indicated wavelengths and M is the fresh weight of the plant material used for anthocyanin extraction.

Anthocyanin composition was profiled based on a previously published HPLC method (Gao et al., 2020) with minor modifications. Briefly, fruits and petioles from wild-type (Rü), as well as gp-1 (YW) fruits transiently expressing pUBQ::FveMYB10L or 35S::FveMYB10, were frozen at -80 °C and freezedried. Samples were homogenized in a solvent solution consisting of 70% methanol, 28% water, and 2% formic acid followed by centrifugation at 15,000 g for 3 min and filtration via a 0.2 μm syringe filter (MicroLiter WHEATON, Millville, NJ, USA). Anthocyanin separation and analyses were done via an Agilent 1200 series HPLC system equipped with a ZORBAX Rapid Resolution StableBond C18 column and a diode-array detector (Agilent, Santa Clara, CA, USA). The binary mobile phase consisted of 5% formic acid in water (solvent A) and 100% methanol (solvent B). Other testing conditions include injection temperature set at 30 °C, flow rate at 1 mL/min, and detection and reference wavelengths at 525 and 650 nm, respectively. The mobile phase composition was 10% B at 0 min, 20% B at 10 min (linear change, same hereinafter), 24% B at 35 min, 60% B between 50 and 60 min, and 10% B at 70 min. Peaks were identified by comparing the chromatograms of the samples to those of known standards including cyanidin-3-glucoside, cyanidin-3,5-diglucoside, pelargonidin-3-glucoside, pelargonidin-3,5-diglucoside, and peonidin-3-glucoside. The fruit and petiole anthocyanin profiling was conducted in triplicate.

# **Light quality treatments**

To test the effect of shade on anthocyanin pigment and gene expression, shade was simulated by supplementing the white light growth condition with constant far-red light (Hydrofarm powerPAR 15-watt LED Bulb, far-red) per 60 x 60 cm<sup>2</sup> to reduce the red/far-red light ratio (Ballaré *et al.*, 1987). WT (Rü) plants were grown in white light (control) and white light supplemented with far-red (shade

treatment). Five replicate plants were grown in each treatment and observed for anthocyanin phenotypes in the fruits and petioles. Petioles and fruits were sampled for anthocyanin content measurement and gene expression analysis with RT-qPCR.

# RNA extraction, cDNA synthesis, and RT-qPCR

For RT-qPCR of endogenous *FveMYB10*, *FveMYB10L*, and anthocyanin biosynthesis genes, total RNA was extracted from white stage fruits or petioles of newly unfolded leaves. White stage fruit was chosen as *FveMYB10* begins expression at this stage (Hawkins *et al.*, 2017), which is also a stage when the fruit metabolites that impede RNA extraction are not yet at a high level. Three fruits or petioles from three individuals were pooled to form one biological sample, and three biological replicates were used. For agrobacterium-infiltrated fruits, total RNA was extracted from the entire fruit at the ripe stage and each infiltrated fruit forms one biological sample.

Tissues were flash-frozen in liquid nitrogen immediately after collection and stored at -80°C until RNA extraction. RNA was extracted following the Cetyl Trimethyl Ammonium Bromide (CTAB) RNA extraction method (Gambino *et al.*, 2008). RNA was reverse transcribed to cDNA using LunaScript RT SuperMix Kit (catalog number E3010, New England Biolabs Inc.), and RT-qPCR was performed using BioRad CFX96 Real-time system and PowerUp SYBR Green Master Mix (catalog number A25742, Applied Biosystems), using a 3-step PCR program (step 1 50°C 2 min, step 2 95°C2 min, step 3 95°C15 sec, step 4 55°C15 sec, step 5 72°C30 sec, repeat steps 3-5 40 cycles). The relative expression level was analyzed using a modified 2-AACT method normalized to the geometric mean of Ct value of the two internal controls (Vandesompele *et al.*, 2002). For genes whose transcripts were undetectable by RT-qPCR, the cycle number was set to 40 for calculation as only 40 cycles were performed for all PCR reactions. For all RT-qPCRs, *F. vesca Protein Phosphatase 2A* (*FvePP2a*; *FvH4\_4g27700*) and *Ubiquitin-conjugating enzyme E2 10* (*FveUBC10*; *FvH4\_7g30920*) were used as the internal controls (Lin-Wang *et al.*, 2014; Caruana *et al.*, 2018). Primers used are listed in Supplementary Table S2.

Student's t test was performed for RT-qPCR of two groups (Fig. 3D). One-way ANOVA followed by Turkey's HSD test was performed for RT-qPCR of multiple groups (Fig. 4C-D and Fig. 5C-D) using the Real Statistics Resource Pack software (Release 7.6).

# In silico analysis of FveMYB10 and FveMYB10L promoters

The promoter sequences (-2000 bp upstream of ATG) of *FveMYB10* and *FveMYB10L* were retrieved from GDR's *F. vesca* Whole Genome v4.0.a1, (https://www.rosaceae.org/), and analyzed in PLANTPAN3.0 (http://plantpan.itps.ncku.edu.tw/) (Chow *et al.*, 2019; Jung *et al.*, 2019) using default parameters in the Multiple Promoter Analysis function.

#### **Results**

# The green petioles-1 locus in F. vesca controls anthocyanin pigment in petioles

A green petioles (gp)-1 mutant was identified from an N-ethyl-N-nitrosourea (ENU) mutagenesis screen performed previously in the YW background (Caruana  $et\ al.$ , 2018) (Materials and Methods). The YW genetic background carries a  $myb10^{w125}$  mutation that causes white fruit (Hawkins  $et\ al.$ , 2016); however, YW still develops normal purple-pigmented petioles (Fig. 1A-B), suggesting that the effect of FveMYB10 is fruit-specific. In addition to an absence of red fruit pigmentation, the newly isolated  $gp-1\ myb10^{w125}$  mutant also lacks purple pigment in the petiole (Fig. 1C). Since gp-1 resembles the  $reduced\ anthocyanins\ in\ petioles\ (rap)$  mutant as well as a natural  $F.\ vesca$  accession FIN12, both of which develop green petioles (Luo  $et\ al.$ , 2018; Castillejo  $et\ al.$ , 2020), complementation tests were conducted to determine whether gp-1 is allelic with rap or FIN12. Reciprocal crosses between rap and gp-1 yielded  $F_1$  progeny with purple petioles (Supplementary Fig. S1), indicating that gp-1 resides in a different gene from rap, which is defective in a GST needed for anthocyanin transport. In contrast,  $F_1$  progeny of a cross between gp-1 pollen and FIN12 stigma still develop green petioles (Fig. 1D-E), suggesting that gp-1 and FIN12 are defective in the same gene that promotes pigmentation in the petiole. However, the identity of the gene affected by gp-1 and FIN12 is unknown.

# Mapping-by-sequencing maps gp-1 to a FveMYB10-like transcription factor

To identify the gene defined by gp-1, a mapping population was constructed by crossing gp-1  $myb10^{w125}$  (YW) with  $GP^+myb10^{w125}$  (H4) that has wild-type petiole pigment. Genomic DNA from 25 F2 green petiole individuals and 25 F2 purple petiole individuals were separately pooled and sequenced using the Illumina platform. Analysis using the SIMPLE pipeline (Wachsman *et al.*, 2017)

narrowed it to 5 candidate genes residing within an 8.65 Mb region of chromosome 1 (Supplementary Fig. S2; Supplementary Table S3). Only one of these, *FveMYB10-Like* (*FveMYB10L*), appeared a strong candidate due to its 57.9% sequence similarity to *FveMYB10*, a known regulator of anthocyanin biosynthesis. In addition, *FveMYB10L* resides near *FveMYB10* on chromosome 1 about 30 KB apart (Fig. 2A). Cloning and sequencing the *FveMYB10L* cDNA corrected its annotation (Supplementary Fig. S3) and showed that the SNP found in *gp-1* resides in the third exon causing a missense mutation (R90K) in *FveMYB10L* (Fig. 2A). The fact that FIN12 harbors a ~100 kb deletion on chromosome 1, deleting both *FveMYB10* and *FveMYB10L* (Fig. 2A, Castillejo *et al.*, 2020) is consistent with its inability to complement *gp-1* (Fig. 1E), lending strong support that *FveMYB10L* is *GP*. Therefore, FIN12 possesses a second independent loss-of-function allele of *FveMYB10L*, confirming the role of *FveMYB10L* in petiole anthocyanin synthesis.

# FveMYB10L falls within a clade of anthocyanin biosynthetic regulators

To compare FveMYB10L with other known anthocyanin biosynthesis regulators, we generated a multiple protein sequence alignment and phylogenetic tree containing FveMYB10L, FveMYB10, and tomato and Arabidopsis MYB transcription factors from R2R3-MYB subgroup 6, which typically regulates anthocyanin biosynthesis (Stracke et al., 2001; Rodrigues et al., 2021) (Fig. 2B). Subgroup 6 MYBs typically have conserved arginine (R), valine (V), and alanine (A) residues and an ANDV motif (indicated by + in Fig. 2C) in the R2-R3 domains which distinguish them from other R2R3 MYBs, although exceptions do occur in the Rosaceae family (Lin-Wang et al., 2010). We also included Arabidopsis and tomato protein sequences from related subgroups 5, 7, and 15. The subgroup 6 MYB proteins, including FveMYB10 and FveMYB10L, form a well-supported clade with 99% bootstrap support. The phylogenetic analysis strongly supports that FveMYB10L belongs to subgroup 6, and not the other related subgroups, indicating a role in anthocyanin synthesis. Moreover, the multiple sequence alignment used to generate this phylogeny indicates that the R90K mutation in gp-1 occurs at a highly conserved arginine (R) residue within the R3 domain (Fig. 2C), converting it to lysine (K). To gain a better understanding of the sequence conservation, multiple alignment of fulllength protein sequences from subgroup 6 MYBs as well as additional sequences from grape and peach is shown in Supplementary Fig. S4. Like FveMYB10, these MYBs show 49-60% similarity at the protein sequence level with FveMYB10L with highest similarity at the R2R3 domain.

# FveMYB10L is not required for fruit coloration

Since qp-1 myb10<sup>W12S</sup> plants develop yellow fruit due to the myb10<sup>W12S</sup> mutation, it is not known if FveMYB10L is also required for the red fruit color. In other words, would a gp-1 single mutant develop red or yellow fruit? Since  $myb10^{W12S}$  is tightly linked to qp-1 (Fig. 2A), we were unable to separate these two mutations via recombination. Hence, we performed a transient expression assay to test if transient expression of wild-type FveMYB10 in qp-1 myb10<sup>W12S</sup> double mutant fruit could rescue the fruit color in the presence of qp-1 mutation. The p35S::FveMYB10 construct from our previous study (Hawkins et al., 2016) was transformed into Agrobacteria, which was infiltrated into qp-1 myb10<sup>W12S</sup> double mutant fruit at white stage by injection (see Materials and Methods). After ~5-10 days, all injected fruits with the p35S::FveMYB10 construct developed red pigmentation in skin and flesh to different extent, a representative image of which is shown in Fig. 3A. The result is similar to prior transient expression experiments showing that p35S::FveMYB10 was able to rescue myb10<sup>W12S</sup> single mutant fruit color (Hawkins et al., 2016; Luo et al., 2018). In contrast, injection of Agrobacteria containing the corresponding empty vector pMDC32 into qp-1 myb10<sup>W125</sup> double mutant fruit had no impact on the fruit color (Fig. 3A). Together, the data indicate that FveMYB10 alone is able to cause red fruit pigment even when FveMYB10L is mutated (i.e. in gp-1 mutant background). Therefore, FveMYB10L function is not required for the fruit coloration and its effect appears specific to the petioles.

# FveMYB10L and FveMYB10 are tissue-specific activators of anthocyanin biosynthesis

Taking advantage of this transient functional assay, we tested whether ectopic over-expression of *FveMYB10L* can activate anthocyanin production in fruits. Anthocyanin production in *gp-1 myb10*<sup>W125</sup> fruits overexpressing *FveMYB10L* would indicate that FveMYB10L, like FveMYB10, can activate anthocyanin biosynthesis, while the same assay using the *FveMYB10L*<sup>R90K</sup> mutant version would test whether this R90K mutation disrupts the ability of *FveMYB10L* to activate anthocyanin biosynthesis. An *Arabidopsis* ubiquitin 10 promoter driven GFP was first constructed in the JH23 vector (Zhou *et al.*, 2021); this *pUBQ::GFP* served as a control construct. Full-length cDNA of wild type *FveMYB10L* as well as mutant *FveMYB10L*<sup>R90K</sup> were PCR amplified and cloned into JH23. Agrobacteria containing *pUBQ::FveMYB10L-GFP*, *pUBQ::FveMYB10L*<sup>R90K</sup> cFFP, or *pUBQ::GFP* were respectively injected into white-stage *gp-1 myb10*<sup>W125</sup> fruits. *pUBQ::FveMYB10L-GFP* injected fruits turned deep red and purple, *pUBQ::FveMYB10*<sup>LR90K</sup> cFFP injected fruits however showed only slight pink, and the *pUBQ::GFP* injected fruits remained the same yellow fruit color (Fig. 3B). Quantification of total

anthocyanin levels in the injected fruits showed that the anthocyanin level in *pUBQ::FveMYB10L-GFP* injected fruits was more than 50-fold higher than that of fruits injected with *FveMYB10L*<sup>R90K</sup>-*GFP* or *pUBQ::GFP*, indicating that the R90K missense mutation greatly reduced the *FveMYB10L* function in anthocyanin biosynthesis (Fig. 3C). The results confirmed that the *gp-1* mutation resides in *FveMYB10L* and that *FveMYB10L*, like *FveMYB10*, can activate anthocyanin biosynthesis.

Since the *myb10*<sup>w125</sup> and *myb10I*<sup>R90K</sup> (*gp-1*) mutations each reduce anthocyanin biosynthesis in only one tissue, we hypothesized that each gene may show tissue-specific expression consistent with its mutant phenotype. We sampled the petioles and fruits of wild type (Rügen) plants and examined the expression of *FveMYB10L* and *FveMYB10* using RT-qPCR. *FveMYB10L* was highly expressed in the petiole but lowly expressed in the fruit (Fig. 3D). In contrast, *FveMYB10* was highly expressed in the fruit but undetectable in the petiole (Fig. 3D). Therefore, these two MYB transcription factors are responsible for anthocyanin biosynthesis in petioles and fruits respectively *in vivo*.

Previous transcriptome work in YW sampled 46 different tissues/stages, not including the petioles (Li et al., 2019). Mining this rich dataset revealed that FveMYB10L expression is barely detectable (<2 TPM) in all tissues sampled, whereas FveMYB10 was mainly detected in reproductive tissues and particularly in the fruit (Supplementary Fig. S5). Taken together with our RT-qPCR in the petioles and fruits, FveMYB10L and FveMYB10 appear to represent petiole- and reproductive-tissue-specific regulators of anthocyanin biosynthesis.

# FveMYB10 and FveMYB10L induce different anthocyanin molecules by differentially activating anthocyanin biosynthesis genes

When *FveMYB10L* was transiently expressed in the strawberry fruits, we noticed that the color hue appears more purple than the red *FveMYB10* overexpressing fruits (Fig. 3A, B), mirroring the difference in hue between the purple petioles and red fruits in wild-type *F. vesca*. Variation in pigment hue is often caused by different types of anthocyanins. We performed HPLC analysis to test whether the anthocyanin composition differed between *gp-1 myb10*<sup>w125</sup> fruits transiently expressing *FveMYB10* and those transiently expressing *FveMYB10L*. We found that *FveMYB10L*-expressing fruits were higher in cyanidin-3,5-diglucoside (peak 1), cyanidin-3-glucoside (peak 3), and peonidin-3-glucoside (peak 5), while *FveMYB10*-expressing fruits are higher in pelargonidin-3-glucoside (peak 4)

(Fig. 4A). We then similarly analyzed wild-type petiole and fruit tissue by HPLC (Fig. 4B). Wild type (Rügen) petioles produced more cyanidin-3,4-diglucoside (peak 1), an unknown peak 2, and peonidin-3-glucoside (peak 5) (Fig. 4B), which resembles the *FveMYB10L*- expressing fruits (Fig. 4A), supporting a role of *FveMYB10L* in petiole. In contrast, pelargonidin (peak 4) that is high in *FveMYB10*-expressing fruit is also high in the Rügen fruits (Fig. 4A, B), supporting the red hue of the fruit. However, peak 3 (cyanidin-3-glucoside) is present at a high level in both petiole and fruit as well as fruits transiently expressing *FveMYB10* or *FveMYB10L* and hence does not appear to be diagnostic between the two MYBs. Taken together, *FveMYB10L* and *FveMYB10* appear to confer distinct anthocyanin compositions characteristic of petiole and fruit respectively.

The above observation suggests that FveMYB10 and FveMYB10L may preferentially activate different anthocyanin biosynthesis genes. To test this hypothesis, we examined the expression of FveDFR1, FveDFR2, and FveUFGT, with DFRs acting in the first committed step that produces anthocyanidins instead of flavonols and UFGT in the last step of anthocyanin biosynthesis (Xu et al., 2014). RNAs were extracted from individual qp-1 myb10<sup>W12S</sup> fruits infiltrated with agrobacteria containing p35S::FveMYB10, pUBQ::FveMYB10L-GFP, or pUBQ::GFP plasmid. RT-qPCR was conducted to first examine transgene expression (Fig. 4C). while the transcripts of GFP or FveMYB10L were only detected in infiltrated fruits with respective plasmid, FveMYB10 transcripts were detected in all fruits but at significantly higher levels in fruits infiltrated with p35S::FveMYB10 (Fig. 4C). This is because the RT-qPCR cannot distinguish the endogenous nonfunctional FveMYB10<sup>W12S</sup> transcripts from FveMYB10 transcripts derived from the transgene. Next, we examined the expression of anthocyanin biosynthesis genes (Fig. 4D). As expected, fruits infiltrated with the pUBQ::GFP containing agrobacterium did not express any anthocyanin biosynthesis genes (Fig. 4D). Interestingly, FveMYB10 actives all three anthocyanin biosynthesis genes with the fruit (#2) that showed a higher FveMYB10 expression expressing a higher level of anthocyanin biosynthesis genes (compare Fig. 4C to 4D). In contrast, FveMYB10L appeared to activate only FveUFGT and FveDFR2 but not FveDFR1 (Fig. 4D). Further, while FveMYB10L and FveMYB10 activated FveDFR2 to similar levels (Fig. 4D), FveMYB10 activated FveUFGT five to six fold higher than FveMYB10L did. Together, the data support that FveMYB10 and FveMYB10L have differential activation preference for anthocyanin biosynthesis genes, qualitatively for FveDFR1 and quantitatively for FveUFGT.

# Expression of FveMYB10L is responsive to change in the red/far-red light ratio

The tissue-specific expression of *FveMYB10* and *FveMYB10L* suggests that these two MYB genes are subject to distinct regulation, responding to tissue-specific or environmental-specific cues. To investigate whether anthocyanin production in fruits and petioles is subject to distinct regulation in response to environmental cues, we tested whether shade could differentially regulate these two MYB genes, since several plant species exhibit reduced anthocyanins in the petiole when under shade (Alokam *et al.*, 2002; Ding *et al.*, 2016). We grew wild type (Rü) plants under white light supplemented with far-red (FR) light, as this reduces the R/FR ratio and mimics shade (Ballaré *et al.*, 1987). After a month, most of the newly formed petioles were completely green, and the plants also exhibited elongated growth (Fig. 5A, B) that is typical of shade avoidance response (Ballaré and Pierik, 2017). Surprisingly, these plants produced red colored fruits (Figure 5A, B), indicating that growth in shade causes reduced anthocyanin production in the petiole but not in the fruit.

To test whether the observed changes in anthocyanin levels may be mediated by *FveMYB10* and *FveMYB10L*, we examined *FveMYB10L* and *FveMYB10* expression in petioles of young leaves and white stage fruits of wild type (Rü) plants. When growing under white light, *FveMYB10L* expression was undetectable in the fruit but highly expressed in the petiole, which is opposite from *FveMYB10* with undetectable expression in the petiole but high expression in the fruit (Fig. 5C). Under simulated shade (white+FR), the expression of *FveMYB10L* in the petiole was about 10-fold lower when compared with that under the white light (Fig. 5C). This shade-mediated repression of *FveMYB10L* expression mirrors the shade-mediated reduction of anthocyanin level in the petiole (Supplementary Fig. S7). In contrast, *FveMYB10* expression level in the fruit does not change much when grown under white light or under the shade (Fig. 5C), suggesting that *FveMYB10* expression is much less sensitive to changes in the light quality. Interestingly, *in silico* analysis of promoter sequences via PlantPAN3.0 (Chow *et al.*, 2019) identified a binding site for the far-red sensing transcription factor *FAR1* in the *FveMYB10L* promoter but not in the *FveMYB10* promoter (Supplementary Fig. S8), supporting that these two MYB genes are regulated differently not only in different tissues but also under different light conditions.

Since the two MYBs differentially regulate downstream anthocyanin biosynthesis genes (Fig. 4D), the anthocyanin biosynthesis genes should also exhibit tissue-specific and light-sensitive expression.

Using RT-qPCR, we examined the expression of *FveUFGT*, *FveDFR1* and *FveDFR2* in the wild type (Rü)

petiole and fruit. *FveDFR1* is not expressed in the petiole (Fig. 5D), consistent with *FveMYB10L's* inability to activate *FveDFR1* in transient expression studies (Fig. 4D). Further, while the petiole-expressed *FveUFGT* and *FveDFR2* are repressed under white+FR (Fig. 5D), the fruit-expressed *FveUFGT* and *FveDFR2* are not repressed under white+FR. Therefore, the tissue- and light- regulated expression pattern of anthocyanin biosynthesis genes mirrors the expression of their respective MYB regulators.

### Discussion

In strawberry, loss of FveMYB10 causes yellow fruit but does not affect the purple color of the petiole (Hawkins et al., 2016; Castillejo et al., 2020), prompting the hypothesis that a petiole-specific MYB transcription factor might exist to regulate anthocyanins in the petiole (Luo et al., 2018). The work reported here suggests that FveMYB10L encodes this proposed petiole-specific MYB transcription factor. Interestingly, both FveMYB10 and FveMYB10L reside in nearby locations on chromosome 1 and likely arose by a gene duplication. Phylogenetic analysis and transient overexpression in fruits revealed that FveMYB10 and FveMYB10L both can activate anthocyanin biosynthesis (Fig. 3 and 4), which is consistent with prior reports that ectopic overexpression of FveMYB10 by the 35S promoter caused elevated anthocyanin pigmentation in leaf tissues (Lin-Wang et al., 2014). Nevertheless, while both MYB genes act to promote anthocyanin biosynthesis, they exhibit somewhat different anthocyanin profiles that are characteristic of petiole and fruit respectively and reflective of their differential regulation of downstream anthocyanin biosynthesis genes. In addition, FveMYB10 and FveMYB10L exhibit distinct tissue-specific expression and mutant phenotypes. FveMYB10 is expressed and acts specifically in the fruit, while FveMYB10L acts specifically in the petiole. The single myb10<sup>W12S</sup> mutant develops yellow fruit but purplish petioles, while a single *qp-1* mutant would develop red fruit but green petioles. Finally, we show that while FveMYB10 expression is not repressed by shade (low R/FR ratio), FveMYB10L expression is dramatically reduced under shade, which corresponds to the formation of green petioles and a reduction of FveMYB10L target genes expression under the shade. Together, our study reveals the existence of two paralogous MYB transcription factors that function in different tissues, activate different targets, and respond differently to environmental signals to confer tissue-specific anthocyanin accumulation as summarized in the model (Fig. 6). The evolution of these two paralogous MYB genes likely offers flexibility in tissue-specific anthocyanin regulation compared to a single MYB10 gene.

The *gp-1* mutant harbors an R90K missense mutation in *FveMYB10L*, while FIN12 possesses a ~100kb deletion encompassing both *FveMYB10* and *FveMYB10L* (Fig. 2A) (Castillejo *et al.*, 2020). However, both mutations confer a green petiole phenotype, and a complementation test between *gp-1* and FIN12 confirmed that they contain mutations in the same gene underlying the green petiole phenotype. Interestingly, both *gp-1* and FIN12 eliminate visible pigment in the petioles despite their harboring different types of mutations. In *gp-1* (R90K), R occurs in a highly conserved region of the R3 domain (Fig. 2C) and is in close proximity to the bHLH domain that enables R2R3 MYBs' interaction with the MBW complex (Heppel *et al.*, 2013). As a result, the R90K mutation in *FveMYB10L* may greatly reduce its function with a similar effect as the deleted *FveMYB10L* in FIN12. We noted a slight pink fruit color when *FveMYB10L* may overexpressed in the fruit (Fig. 3B), suggesting some residual activities of *FveMYB10L* only observable when *FveMYB10L* response was overexpressed in the transient system.

FveMYB10 and FveMYB10L confer distinct anthocyanin composition to the fruits and petioles, likely due to their differential activation of downstream anthocyanin biosynthesis genes including FveUFGT and FveDFR1. While there are only limited differences between FveMYB10 and FveMYB10L in the R2 and R3 DNA binding motifs (Fig. 2C), there are significant differences outside the R2R3 domain (Fig. S6), which could contribute to their differential binding of downstream targets.

Moreover, while both MYBs can activate FveDFR2, only FveMYB10 could activate FveDFR1 in the transient system (Fig. 4D). The altered expression levels of FveDFR1 and FveDFR2 were previously shown to cause changes in the hydroxylation patterns of anthocyanins in strawberry fruit due to their different substrate specificities (Miosic et al., 2014). Specifically, only FveDFR1 can act on dihydrokaempferol, the precursor to pelargonidin-3-glucoside, which is consistent with our detection of higher pelargonidin-3-glucoside levels in FveMYB10-overexpressing fruits than in FveMYB10L-overexpressing fruits. Therefore, differential activation of FveDFRs by tissue-specific MYBs likely underlies the observed differences in hue and anthocyanin composition between fruit and petiole tissues.

In addition to their tissue-specific effects on anthocyanin intensity and composition, *FveMYB10* and *FveMYB10L* differ in their response to environmental cues, specifically light quality. We found that *FveMYB10L*, but not *FveMYB10*, is downregulated under low R/FR ratio, which simulates shade.

Accordingly, petiole looks green in color and petiole anthocyanin level is reduced (Fig. 5B and S7). Consistent with a function in photoprotection, vegetative anthocyanin production is often light-inducible and absorbs light in the range of photosynthetically active radiation (Close and Beadle, 2003; Albert *et al.*, 2009; Gould *et al.*, 2010). In contrast, fruit pigmentation is thought to attract frugivores for seed dispersal, although this function has not been explicitly tested in strawberry (Lomascolo *et al.*, 2010; Nevo *et al.*, 2018). *FveMYB10* expression that is not repressed under our shade condition may allow anthocyanins to be synthesized in fruits even in the shade to attract seed dispersers. We note that previous studies find light-regulation of FveMYB10, with dark-grown apple and strawberry fruits failing to accumulate anthocyanins (Takos *et al.*, 2006; Xu *et al.*, 2018; Li *et al.*, 2020); however, these prior studies compare light and dark treatments, while ours compares white light treatments with or without far-red supplementation and is therefore testing the effects of light quality. The ability to separately regulate petiole *FveMYB10L* and fruit *FveMYB10* may provide flexibility in regulating anthocyanin production for different biological functions. The detection of a FAR1-binding site in the promoter of *FveMYB10L* but not *FveMYB10* lays the foundation for future investigations into the mechanism underlying differential regulations of *FveMYB10* and *FveMYB10L*.

Tissue- and environment-specific regulation of anthocyanin biosynthesis by duplicate MYBs was also reported in other plant species, suggesting a common need to decouple the regulation of pigment synthesis between fruit and vegetative tissues. In tomato, two MYBs, *SIANT1* and *SIAN2*, upregulate anthocyanin contents when ectopically overexpressed, but only *SIAN2* is specifically upregulated under cold and high light conditions (Matus *et al.*, 2017). In grape, two clusters of MYBs regulate anthocyanin biosynthesis in fruits and vegetative tissues respectively; when both clusters were ectopically expressed, they caused anthocyanin biosynthesis in hairy roots and affected anthocyanin composition by regulating F3'5'H differentially (Matus *et al.*, 2017). Finally, a vegetative tissue-specific MYB10.4, distinct from the fruit-specific MYB10.2, is involved in the red leaf color of an ornamental peach cultivar (Zhou *et al.*, 2014). These MYBs show 49-60% similarity at the protein sequence level with FveMYB10L (Supplementary Fig. S4). Together with our current work in strawberry, it appears that separately regulated paralogous MYBs with different downstream target specificity may have frequently evolved to offer flexibility and advantages to plants under changing environments.

# Acknowledgements

We would like to thank Dr. Courtney Hollender and Ms. Aviva Geretz for the ENU mutagenesis, Dr. Fuxi Wang for initially identifying the *gp-1* mutant, and Dr. Chunying Kang for the *rap-1* seeds. We also thank Daniel Pearlstein for technical assistance with anthocyanin analysis.

#### **Author Contributions**

M.P., X.L., and Z.L. designed experiments, M.P., X.L., Z.T., K.M., and L.G. performed experiments, T.H., Y.L., and Z. L. supervised and supported the project, M.P., X.L., and Z.L. wrote the manuscript. X.L. and M.P. contributed equally. All authors commented on the manuscript.

### **Conflict of interest**

No conflict of interest declared.

# **Funding**

The work was supported by the Maryland Summer Scholars Award to M.P., NSF grants (IOS1444987 and IOS1935169) to Z. L., and the Maryland Agricultural Experiment Station Hatch Project MD-CBMG-19008 to Z. L.

# Data availability

The genome resequencing data used for mapping the *gp-1* mutation are available from the Sequence Read Archive (SRA) at NCBI associated with BioProject PRJNA823731.

# **Figure Legends**

# Figure 1. Characterization of gp-1 mutant in F. vesca.

(A-C) Whole plant, fruit, and petioles of WT (Rü) (A),  $myb10^{w125}$  (YW) (B), and gp-1  $myb10^{w125}$  (YW) double mutant (C). (D) A FIN12 adult plant. (E) Complementation result between FIN12 and gp-1, showing an F1 progeny with green petioles. Scale bars: 8 mm.

# Figure 2. Phylogenetic analysis of some MYBs with roles in anthocyanin biosynthesis.

(A) Diagram of a chromosome 1 region corresponding to a large deletion in FIN12 that contains the *FveMYB10* (FvH4\_1g22020) and *FveMYB10-like* (FvH4\_1g22040) genes. (B) Rooted maximum likelihood phylogeny containing FveMYB10, FveMYB10-like, and MYBs from subgroup 6 and related subgroups in *Arabidopsis* and tomato. Clades corresponding to subgroups are indicated by labeled arrows. Numbers at each node indicate percent bootstrap support from 1000 replicates. (C) Multiple sequence alignment containing protein sequences of R2R3 domains of FveMYB10, FveMYB10-Like, and subgroup 6 MYB transcription factors in tomato and *Arabidopsis*. The boxed W indicates a conserved tryptophan that is converted to serine (S) in *myb10*<sup>W125</sup>; the boxed R indicates a conserved arginine that is converted to lysine (K) in *gp-1*. Residues conserved among all WT sequences are marked with an asterisk. R2, R3, and bHLH domains are based on a prior study (Heppel *et al.*, 2013). + sign indicates residues diagnostic for subgroup 6 MYBs (Lin-Wang *et al.*, 2010).

# Figure 3. Transient over-expression of *FveMYB10* or *FveMYB10L* but not *FveMYB10L* activates anthocyanin biosynthesis in fruit.

(A) *gp-1 myb10*<sup>W125</sup> mutant fruits infiltrated with Agrobacteria containing *p35S::FveMYB10* (right) or *pMDC32* empty vector (left). (B) *gp-1 myb10*<sup>W125</sup> mutant fruits respectively infiltrated with Agrobacteria containing *pUBQ::FveMYB10L-GFP*, *pUBQ::FveMYB10L*<sup>R90K</sup>-*GFP*, or *pUBQ::GFP*. Representative fruit images are shown. (C) Total anthocyanin content quantification of fruits derived from (B) above. Data are means (±SD) of three technical replicates. Y-axis is the total anthocyanin content calculated as [A530–(0.25×A657)]/M. Two biological replicates were conducted with similar results. (D) RT-qPCR quantification of *FveMYB10* and *FveMYB10L* transcripts in the petiole and fruit of WT (Rü) plants. Y-axis is the relative expression level against two internal controls *FvePP2a* (FvH4\_4g27700) and *FveUBC10* (FvH4\_7g30920), data are means (±SD) of three technical replicates.

Significant difference between petiole and fruit is marked by \*\* (P < 0.001 by two-tailed Student's test). Three biological replicates were conducted with similar results. Scale bars in (A) and (B) are 8 mm.

# Figure 4. Anthocyanin profiles and biosynthesis gene expression in fruits transiently expressing FveMYB10 and FveMYB10L

(A) The anthocyanin profiles of fruits transiently over-expressing *FveMYB10L* (red) or *FveMYB10* (blue). Insert is a zoom-in of peaks 4-5. (B) The anthocyanin profile of petiole (black) and fruit (purple). The chemical identity of each peak for (A) and (B) is shown in the insert of (B). Three replicates all show similar profiles and one such replicate is shown here. (C) RT-qPCR results showing over-expressed *FveMYB10, FveMYB10L-GFP*, and *GFP* in respective infiltrated fruits. Results of two independently infiltrated fruits (#1 and #2) are shown. (D) RT-qPCR results testing activation of anthocyanin biosynthesis genes by the over-expressed *GFP, FveMYB10* and *FveMYB10L-GFP*. Data are from the same two independently infiltrated fruits (#1 and #2) as (C). Statistically significant differences among different samples for the same gene are indicated by different letters (p-value <0.05 by one-way ANOVA followed by Turkey's HSD test).

# Figure 5. Petiole and fruit phenotype and anthocyanin biosynthesis gene expression under different light conditions

(A-B) WT (Rü) plants grown under white light (A) and simulated shade (white + FR) (B). Fruits are indicated with an arrow. One representative plant from 5 replicates is shown. (C) RT-qPCR quantification of *FveMYB10L* and *FveMYB10* transcripts in WT (Rü) petiole and fruit under different light conditions. (D) RT-qPCR quantification of anthocyanin biosynthesis genes in WT (Rü) petiole and fruit under different light conditions. Y-axis indicates the relative expression level against two internal controls *FvePP2a* and *FveUBC10*; data are means (±SD) of three technical replicates. Statistically significant differences among different samples/conditions for the same gene are indicated by different letters (p-value <0.05 by one-way ANOVA followed by Turkey's HSD test). Three white stage fruits or young leaf petioles from three individual plants in each light condition were pooled to form a biological replicate. Three biological replicates were conducted with similar results. Scale bars are 8 mm.

# Figure 6. A model summarizing the roles of *FveMYB10* and *FveMYB10L* in fruit and petiole under different light conditions

When the wild strawberry is grown under white light conditions (left) with a high R/FR (red/far-red) ratio, *FveMYB10L* and *FveMYB10* are expressed in petioles and fruits respectively, activating different anthocyanin biosynthesis genes and contributing to different color hues in the petiole and fruit. When the plant is growing under the shade (right) with a low the R/RF ratio, *FveMYB10L* expression in the petiole is reduced, causing the green color petiole due to a lack of anthocyanin biosynthesis. However, *FveMYB10* expression in the fruit is not repressed and red color fruit is still formed.

#### Reference

- Albert NW, Lewis DH, Zhang H, Irving LJ, Jameson PE, Davies KM. 2009. Light-induced vegetative anthocyanin pigmentation in Petunia. Journal of Experimental Botany **60**, 2191–2202.
- **Alokam S, Chinnappa CC, Reid DM**. 2002. Red/far-red light mediated stem elongation and anthocyanin accumulation in Stellaria longipes: differential response of alpine and prairie ecotypes. Canadian Journal of Botany **80**, 72–81.
- **Ballaré CL, Pierik R**. 2017. The shade-avoidance syndrome: multiple signals and ecological consequences. Plant, Cell & Environment **40**, 2530–2543.
- **Ballaré CL, Sánchez RA, Scopel AL, Casal JJ, Ghersa CM**. 1987. Early detection of neighbour plants by phytochrome perception of spectral changes in reflected sunlight. Plant, Cell & Environment **10**, 551–557.
- Berardini TZ, Reiser L, Li D, Mezheritsky Y, Muller R, Strait E, Huala E. 2015. The Arabidopsis Information Resource: Making and Mining the Gold Standard Annotated Reference Plant Genome. Genesis (New York, N.Y.: 2000) 53, 474–485.
- Caruana JC, Sittmann JW, Wang W, Liu Z. 2018. Suppressor of Runnerless Encodes a DELLA Protein that Controls Runner Formation for Asexual Reproduction in Strawberry. Molecular Plant 11, 230–233.
- Castillejo C, Waurich V, Wagner H, et al. 2020. Allelic Variation of MYB10 Is the Major Force Controlling Natural Variation in Skin and Flesh Color in Strawberry (Fragaria spp.) Fruit. The Plant Cell 32, 3723–3749.
- **Chalker-Scott L**. 1999. Environmental Significance of Anthocyanins in Plant Stress Responses. Photochemistry and Photobiology **70**, 1–9.
- Chen S, Zhou Y, Chen Y, Gu J. 2018. fastp: an ultra-fast all-in-one FASTQ preprocessor. Bioinformatics 34, i884–i890.
- Chow C-N, Lee T-Y, Hung Y-C, Li G-Z, Tseng K-C, Liu Y-H, Kuo P-L, Zheng H-Q, Chang W-C. 2019. PlantPAN3.0: a new and updated resource for reconstructing transcriptional regulatory networks from ChIP-seq experiments in plants. Nucleic Acids Research 47, D1155–D1163...
- Close DC, Beadle CL. 2003. The Ecophysiology of Foliar Anthocyanin. The Botanical Review 69, 149–161.
- Curtis MD, Grossniklaus U. 2003. A Gateway Cloning Vector Set for High-Throughput Functional Analysis of Genes in Planta. Plant Physiology 133, 462–469.
- **Ding Z, Zhang Y, Xiao Y, et al.** 2016. Transcriptome response of cassava leaves under natural shade. Scientific Reports **6**, 31673.
- **Edgar RC**. 2004. MUSCLE: a multiple sequence alignment method with reduced time and space complexity. BMC Bioinformatics **5**, 113.
- **Edger PP, VanBuren R, Colle M, et al.** 2018. Single-molecule sequencing and optical mapping yields an improved genome of woodland strawberry (Fragaria vesca) with chromosome-scale contiguity. GigaScience 7.

- **Fernandez-Pozo N, Menda N, Edwards JD, et al.** 2015. The Sol Genomics Network (SGN)—from genotype to phenotype to breeding. Nucleic Acids Research **43**, D1036–D1041.
- **Gambino G, Perrone I, Gribaudo I**. 2008. A Rapid and effective method for RNA extraction from different tissues of grapevine and other woody plants. Phytochemical analysis: PCA **19**, 520–525.
- Gao Q, Luo H, Li Y, Liu Z, Kang C. 2020. Genetic modulation of RAP alters fruit coloration in both wild and cultivated strawberry. Plant Biotechnology Journal 18, 1550–1561.
- **Gaston A, Osorio S, Denoyes B, Rothan C**. 2020. Applying the Solanaceae Strategies to Strawberry Crop Improvement. Trends in Plant Science **25**, 130–140.
- **Gould KS, Dudle DA, Neufeld HS**. 2010. Why some stems are red: cauline anthocyanins shield photosystem II against high light stress. Journal of Experimental Botany **61**, 2707–2717.
- Hawkins C, Caruana J, Li J, Zawora C, Darwish O, Wu J, Alkharouf N, Liu Z. 2017. An eFP browser for visualizing strawberry fruit and flower transcriptomes. Horticulture Research 4, 1–8.
- **Hawkins C, Caruana J, Schiksnis E, Liu Z**. 2016. Genome-scale DNA variant analysis and functional validation of a SNP underlying yellow fruit color in wild strawberry. Scientific Reports **6**.
- Heppel SC, Jaffé FW, Takos AM, Schellmann S, Rausch T, Walker AR, Bogs J. 2013. Identification of key amino acids for the evolution of promoter target specificity of anthocyanin and proanthocyanidin regulating MYB factors. Plant Molecular Biology 82, 457–471.
- Joldersma D, Sadowski N, Timp W, Liu Z, Joldersma D, Sadowski N, Timp W, Liu Z. 2022. Assembly and annotation of *Fragaria vesca* \_Yellow Wonder genome, a model diploid strawberry for molecular genetic research. Fruit Research 2, 1–5.
- **Jones DT, Taylor WR, Thornton JM**. 1992. The rapid generation of mutation data matrices from protein sequences. Bioinformatics **8**, 275–282.
- **Jung S, Lee T, Cheng C-H, et al.** 2019. 15 years of GDR: New data and functionality in the Genome Database for Rosaceae. Nucleic Acids Research 47, D1137–D1145.
- **Justice MJ, Noveroske JK, Weber JS, Zheng B, Bradley A**. 1999. Mouse ENU Mutagenesis. Human Molecular Genetics **8**, 1955–1963.
- **King MC, Cliff MA.** 2002. Development of a model for prediction of consumer liking from visual attributes of new and established apple cultivars. Journal American Pomological Society **56**, 223-229.
- **Kong J-M, Chia L-S, Goh N-K, Chia T-F, Brouillard R**. 2003. Analysis and biological activities of anthocyanins. Phytochemistry **64**, 923–933.
- **Landi M, Tattini M, Gould KS**. 2015. Multiple functional roles of anthocyanins in plant-environment interactions. Environmental and Experimental Botany **119**, 4–17.
- **Li P, Li Y-J, Zhang F-J, Zhang G-Z, Jiang X-Y, Yu H-M, Hou B-K**. 2017. The Arabidopsis UDP-glycosyltransferases UGT79B2 and UGT79B3, contribute to cold, salt and drought stress tolerance via modulating anthocyanin accumulation. The Plant Journal: For Cell and Molecular Biology **89**, 85–103.
- **Li Y, Pi M, Gao Q, Liu Z, Kang C**. 2019. Updated annotation of the wild strawberry Fragaria vesca V4 genome. Horticulture Research **6**, 1–9.
- Li Y, Xu P, Chen G, Wu J, Liu Z, Lian H. 2020. FvbHLH9 Functions as a Positive Regulator of

- Anthocyanin Biosynthesis by Forming a HY5-bHLH9 Transcription Complex in Strawberry Fruits. Plant and Cell Physiology **61**, 826–837.
- Lin-Wang K, Bolitho K, Grafton K, Kortstee A, Karunairetnam S, McGhie TK, Espley RV, Hellens RP, Allan AC. 2010. An R2R3 MYB transcription factor associated with regulation of the anthocyanin biosynthetic pathway in Rosaceae. BMC Plant Biology 10, 50.
- Lin-Wang K, McGhie TK, Wang M, Liu Y, Warren B, Storey R, Espley RV, Allan AC. 2014. Engineering the anthocyanin regulatory complex of strawberry (Fragaria vesca). Frontiers in Plant Science 5.
- Liu Z, Ma H, Jung S, Main D, Guo L. 2020. Developmental mechanisms of fleshy fruit diversity in Rosaceae. Annual review of plant biology 71, 547–573.
- **Lomascolo SB, Levey DJ, Kimball RT, Bolker BM, Alborn HT**. 2010. Dispersers shape fruit diversity in Ficus (Moraceae). Proceedings of the National Academy of Sciences **107**, 14668–14672.
- **Luo H, Dai C, Li Y, Feng J, Liu Z, Kang C**. 2018. Reduced Anthocyanins in Petioles codes for a GST anthocyanin transporter that is essential for the foliage and fruit coloration in strawberry. Journal of Experimental Botany **69**, 2595–2608.
- Madeira F, Pearce M, Tivey ARN, Basutkar P, Lee J, Edbali O, Madhusoodanan N, Kolesnikov A, Lopez R. 2022. Search and sequence analysis tools services from EMBL-EBI in 2022. Nucleic acids research, gkac240.
- Matus JT, Cavallini E, Loyola R, et al. 2017. A group of grapevine MYBA transcription factors located in chromosome 14 control anthocyanin synthesis in vegetative organs with different specificities compared with the berry color locus. The Plant Journal 91, 220–236.
- Medina-Puche L, Cumplido-Laso G, Amil-Ruiz F, Hoffmann T, Ring L, Rodríguez-Franco A, Caballero JL, Schwab W, Muñoz-Blanco J, Blanco-Portales R. 2014. MYB10 plays a major role in the regulation of flavonoid/phenylpropanoid metabolism during ripening of Fragaria × ananassa fruits. Journal of Experimental Botany 65, 401–417.
- Miosic S, Thill J, Milosevic M, Gosch C, Pober S, Molitor C, Ejaz S, Rompel A, Stich K, Halbwirth H. 2014. Dihydroflavonol 4-Reductase Genes Encode Enzymes with Contrasting Substrate Specificity and Show Divergent Gene Expression Profiles in Fragaria Species. PLOS ONE 9, e112707.
- Nevo O, Valenta K, Razafimandimby D, Melin AD, Ayasse M, Chapman CA. 2018. Frugivores and the evolution of fruit colour. Biology Letters 14, 20180377.
- **Pojer E, Mattivi F, Johnson D, Stockley CS**. 2013. The Case for Anthocyanin Consumption to Promote Human Health: A Review. Comprehensive Reviews in Food Science and Food Safety **12**, 483–508.
- **Rodrigues JA, Espley RV, Allan AC**. 2021. Genomic analysis uncovers functional variation in the C-terminus of anthocyanin-activating MYB transcription factors. Horticulture Research **8**, 1–14.
- **Stecher G, Tamura K, Kumar S**. 2020. Molecular Evolutionary Genetics Analysis (MEGA) for macOS. Molecular Biology and Evolution **37**, 1237–1239.
- **Stracke R, Werber M, Weisshaar B**. 2001. The R2R3-MYB gene family in Arabidopsis thaliana. Current Opinion in Plant Biology **4**, 447–456.

- Sun C, Deng L, Du M, Zhao J, Chen Q, Huang T, Jiang H, Li C-B, Li C. 2020. A Transcriptional Network Promotes Anthocyanin Biosynthesis in Tomato Flesh. Molecular Plant 13, 42–58.
- **Takos MA, Robinson PS, Walker RA**. 2006. Transcriptional regulation of the flavonoid pathway in the skin of dark-grown <u>Cripps</u> Red apples in response to sunlight. The Journal of Horticultural Science and Biotechnology **81**, 735–744.
- **Tanaka Y, Sasaki N, Ohmiya A**. 2008. Biosynthesis of plant pigments: anthocyanins, betalains and carotenoids. The Plant Journal **54**, 733–749.
- Vandesompele J, De Preter K, Pattyn F, Poppe B, Van Roy N, De Paepe A, Speleman F. 2002. Accurate normalization of real-time quantitative RT-PCR data by geometric averaging of multiple internal control genes. Genome Biology 3, research0034.1.
- Wachsman G, Modliszewski JL, Valdes M, Benfey PN. 2017. A SIMPLE Pipeline for Mapping Point Mutations. Plant Physiology 174, 1307–1313.
- **Xu W, Dubos C, Lepiniec L**. 2015. Transcriptional control of flavonoid biosynthesis by MYB-bHLH-WDR complexes. Trends in Plant Science **20**, 176–185.
- Xu W, Peng H, Yang T, Whitaker B, Huang L, Sun J, Chen P. 2014. Effect of calcium on strawberry fruit flavonoid pathway gene expression and anthocyanin accumulation. Plant Physiology and Biochemistry 82, 289–298.
- Xu P, Zawora C, Li Y, Wu J, Liu L, Liu Z, Cai R, Lian H. 2018. Transcriptome sequencing reveals role of light in promoting anthocyanin accumulation of strawberry fruit. Plant Growth Regulation 86, 121–132.
- **Zhang Y, Butelli E, Martin C**. 2014. Engineering anthocyanin biosynthesis in plants. Current Opinion in Plant Biology **19**, 81–90.
- **Zhou J, Sittmann J, Guo L, Xiao Y, Huang X, Pulapaka A, Liu Z**. 2021. Gibberellin and auxin signaling genes RGA1 and ARF8 repress accessory fruit initiation in diploid strawberry. Plant Physiology **185**, 1059–1075.
- **Zhou J, Wang G, Liu Z**. 2018. Efficient genome editing of wild strawberry genes, vector development and validation. Plant Biotechnology Journal **16**, 1868–1877.
- **Zhou Y, Zhou H, Kui L-W, Vimolmangkang S, Espley RV, Lu Wang, Allan AC, Yuepeng Han.** 2014. Transcriptome analysis and transient transformation suggest an ancient duplicated MYB transcription factor as a candidate gene for leaf red coloration in peach. BMC Plant Biology **14**, 299–325.
- Zhu Q, Yu S, Zeng D, et al. 2017. Development of —Preple Endosperm Rice" by Engineering Anthocyanin Biosynthesis in the Endosperm with a High-Efficiency Transgene Stacking System. Molecular Plant 10, 918–929.

Figure 1

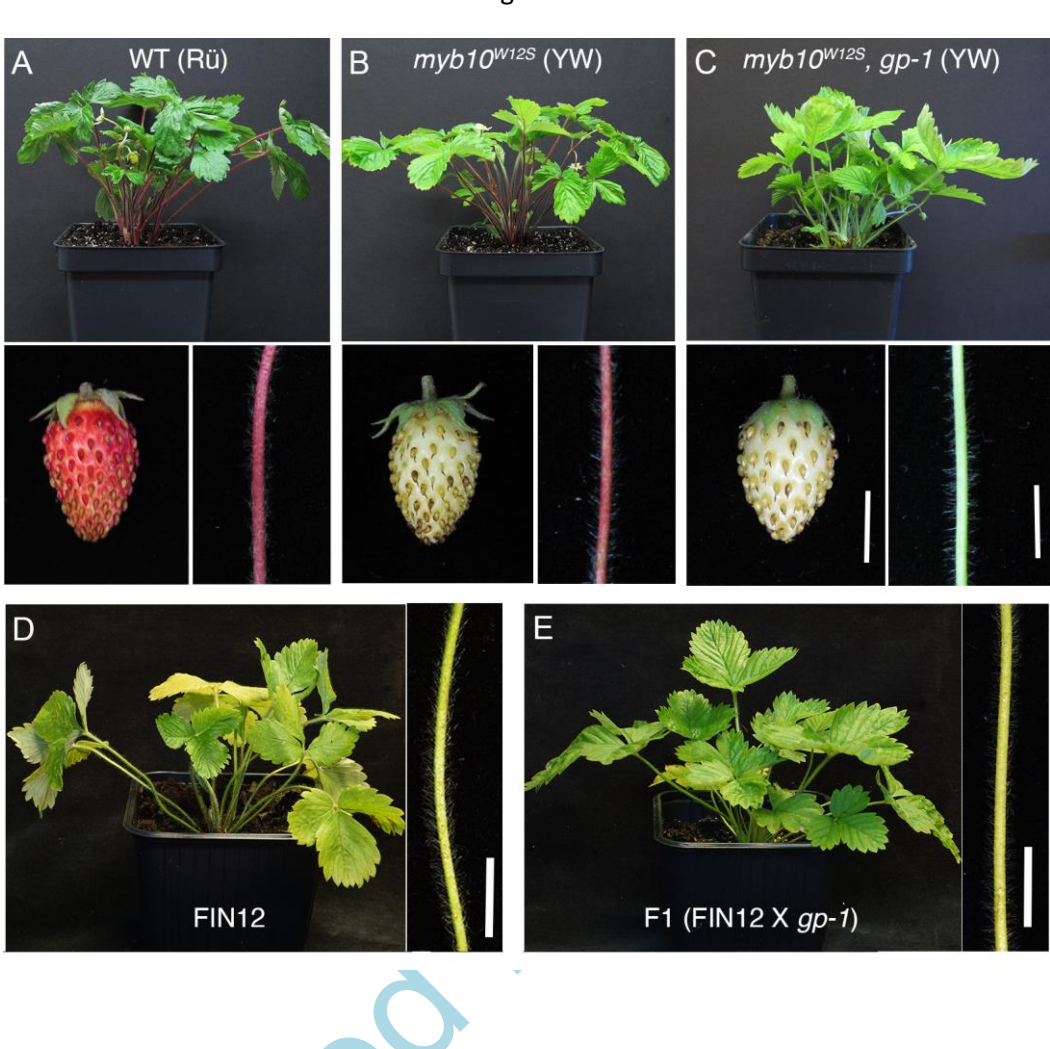
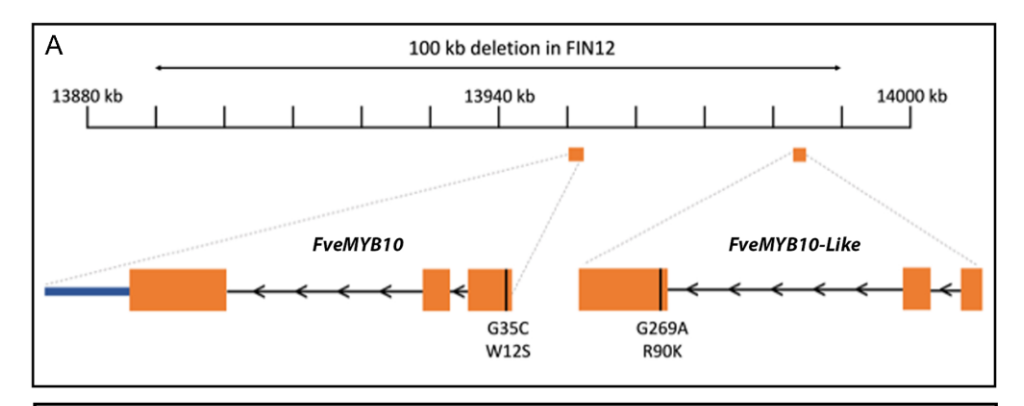
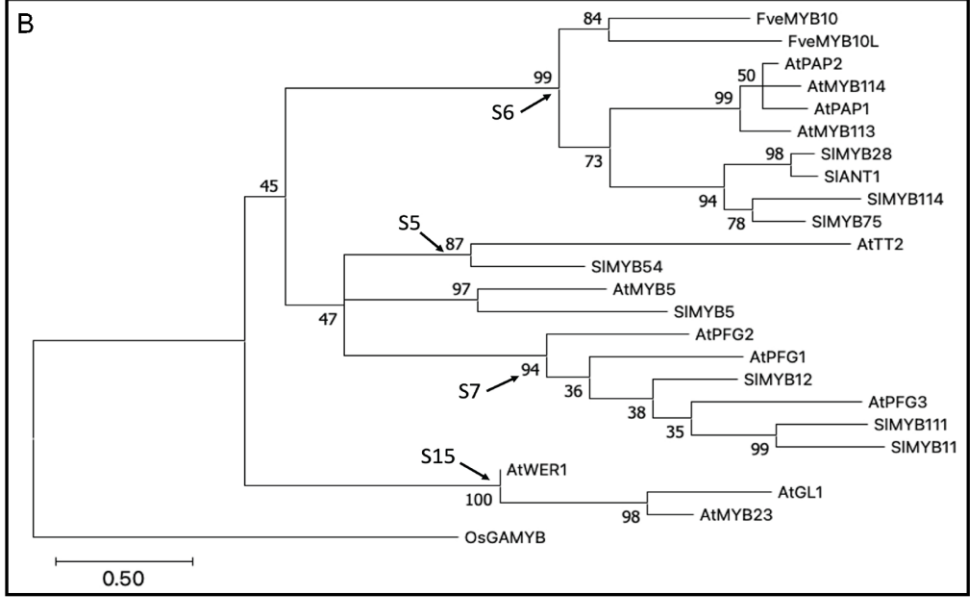


Figure 2





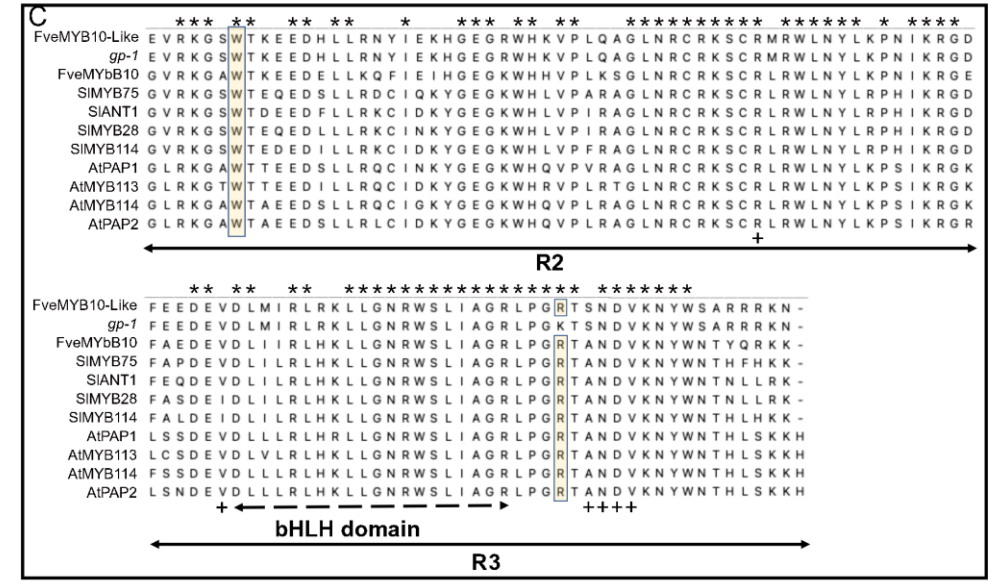




Figure 3

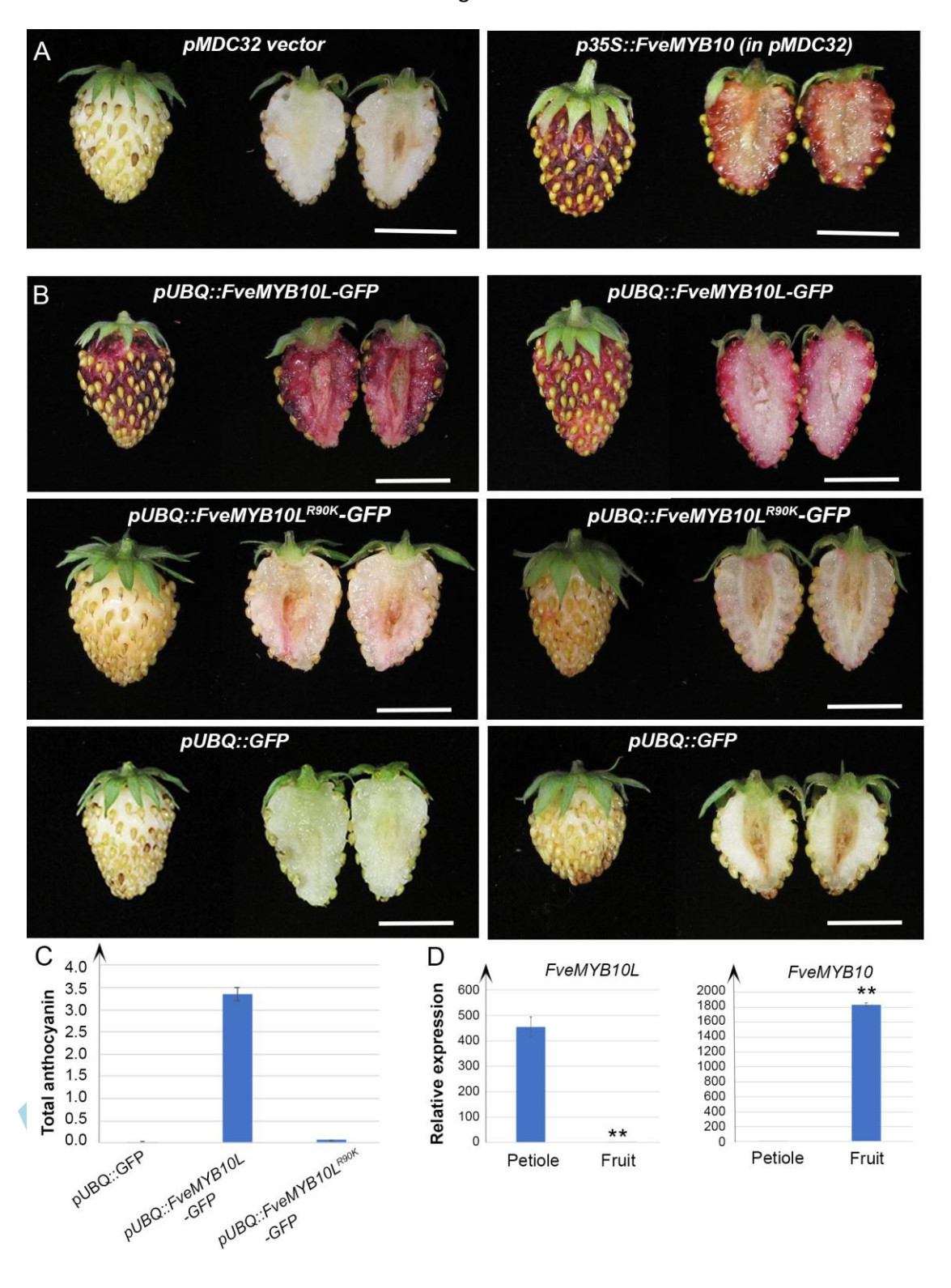


Figure 4

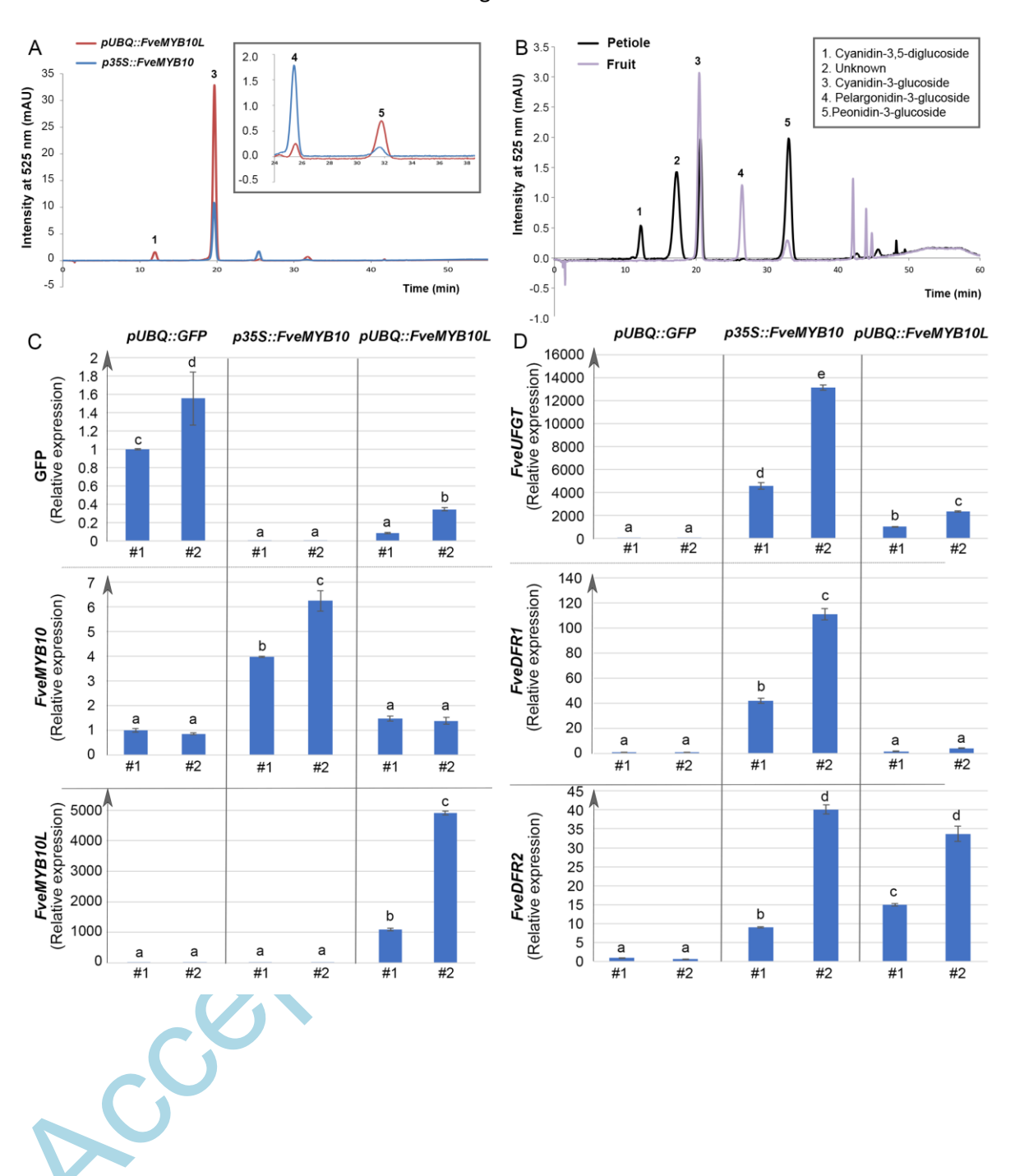


Figure 5

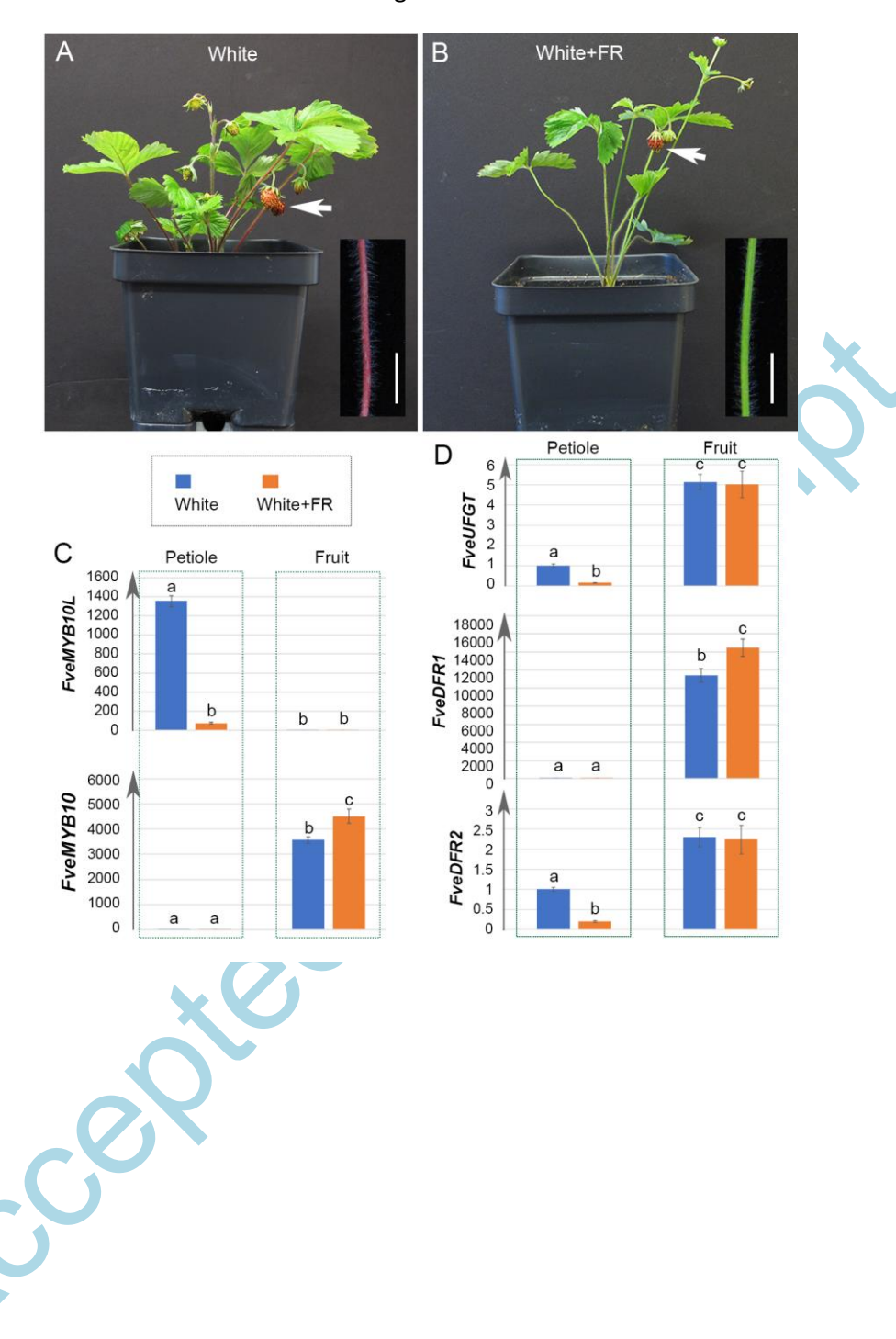


Figure 6

